

Collinear Cluster Tri-Partition as a Probe of Clustering in Heavy Nuclei

D. V. Kamanin, A. A. Alexandrov, I. A. Alexandrova, N. A. Kondatyev,
E. A. Kuznetsova, O. V. Strekalovsky, V. E. Zhuchko, Yu. V. Pyatkov,
W. von Oertzen, Yu. E. Lavrova, A. N. Tyukavkin, O. V. Falomkina,
N. Jacobs, V. Malaza and Yu. V. Ryabov

1 Introduction

Nuclear fission, a process where a heavy nucleus decays into two fragments of intermediate mass (e.g., Ba + Kr) has been identified by Hahn and Strassmann in 1938. It was discovered by chemical analysis while irradiating natural uranium with thermal neutrons [1]. Shortly afterwards Petrzhak and Flerov [2] observed spontaneous fission of the ^{238}U isotope. The energy release in the fission process was immediately calculated by all leading physicists at that time to be very large, typically 200–205 MeV (e.g., Meitner and Frisch [3]). The large value is due to the larger binding energy per nucleon (E_B/N) in the mass range around mass $A = 54$ (iron, $E_B/N = 8.2\text{ MeV}$), as compared to the value at the end of the periodic table, $E_B/N = 7.2\text{ MeV}$. This fact could have been noticed four years before these discoveries, because of the existence of the liquid-drop model and the nuclear-mass

D. V. Kamanin (✉) · A. A. Alexandrov · I. A. Alexandrova · N. A. Kondatyev ·
E. A. Kuznetsova · O. V. Strekalovsky · V. E. Zhuchko · Y. V. Pyatkov · O. V. Falomkina
Joint Institute for Nuclear Research, Dubna 141980, Russia
e-mail: kamanin@jinr.ru

Y. V. Pyatkov · Y. E. Lavrova · A. N. Tyukavkin
National Nuclear Research University MEPhI, Moscow 115409, Russia

W. von Oertzen
Helmholtz-Zentrum Berlin, Glienickerstr. 100, 14109 Berlin, Germany

O. V. Falomkina
Physics Faculty, Computer Methods in Physics Division,
Lomonosov Moscow State University, Moscow 119899, Russia

N. Jacobs · V. Malaza
Faculty of Military Science, Military Academy, University of Stellenbosch,
Saldanha 7395, South Africa

Y. V. Ryabov
Institute for Nuclear Research RAN, Moscow 117312, Russia

formula of Bethe and Weizsäcker [4]. However, the large collective motion through a large deformation (today called super-deformation) was considered to be unlikely. The fission of heavy low-excited nuclei into three fragments of comparable masses, so called “true ternary fission”, has been intensively investigated soon after the discovery of fission. Swiatecki [5] has shown within the framework of the liquid-drop model that fission into three heavy fragments is energetically more favorable than binary fission for all nuclei with fission parameters $30.5 < Z^2/A < 43.3$. In 1963 Strutinsky [6] has calculated the equilibrium shapes of the fissioning nucleus and has shown that along with the ordinary configuration with one neck, there is the possibility of more complicated elongated configurations with two and even three necks; at the same time it was stressed that such configurations are much less probable. Later, Diehl and Greiner [7, 8] have shown a preference for prolate over oblate saddle point shapes for the fission of a nucleus into three fragments of similar size. Such prescission configurations could lead to an almost collinear separation of the decay partners, at least in a sequential fission process. Actually, the Coulomb interaction in the total potential energy is the smallest for the linear arrangements of the three fragments. Furthermore, results demonstrating a decisive role of shell effects in the formation of the multi-body chain-like nuclear molecules were obtained also by Poenaru et al. [9]. On the experimental side there have been multiple attempts to find the true ternary fission in low-energy fission by means of counting techniques and in radiochemical studies. The schemes of the spectrometric experiments were based on the assumption of comparable angles between all three fragments emitted [10, 11]. Masses of the fragments were calculated in this case based on experimental values of the energies and angles. Contradictory results have been obtained; these were treated as showing the absence of fission fragments in the vicinity of mass fifty both in binary and ternary fission [12]. At the same time almost collinear ternary decays of excited heavy nuclear systems were known from the experiments in refs. [13, 14] at the early stage of our work. Bearing in mind the results mentioned above, we came to the conclusion, that collinear tri-partition of low excited heavy nuclear systems would be a promising field of research. In our first experiments dedicated to this problem [15, 16] some indications of such processes were already observed. At least one of the decay products detected was a magic nucleus. By analogy with the known cluster decay (or lead radioactivity), the process has been called “collinear cluster tri-partition” (CCT).

2 “Ni”-Bump and Its Internal Structure

We report here some results of three different experiments (marked Ex1, Ex2, Ex3 below) devoted to the search for collinear cluster tri-partition of ^{252}Cf (sf) and performed in the Flerov Laboratory of Nuclear Reactions (FLNR) of the Joint Institute for Nuclear Research (JINR) in Dubna. The TOF-E (time-of-flight vs. energy) method for the measurements of two FF masses in coincidence with detectors placed at 180° was used in all three experiments. In this method, the fragment velocities

V , obtained by means of TOF and the energy E are measured for each detected fragment individually. Only two fragments were actually detected in each fission event (in two detectors, at 1800) and their total mass, the sum M_s will serve as a sign of a multi-body decay, if it is significantly smaller than the mass of the initial system (“missing mass” method).

In the first experiment (Ex1) performed at the FOBOS [17] set-up about 13×10^6 coincident binary fission events have been collected. It has the highest statistics among all three experiments discussed here. The TOF of the fragment has been measured over a flight path of 50 cm between the “start” detector which is based on micro-channel plates (MCP) placed next to the ^{252}Cf source and the “stop” detectors formed by position sensitive avalanche counters (PSAC). The energies of those coincident fragments, which passed through the PSACs, were measured in the Bragg ionization chambers.

In the second experiment (Ex2), due to the low yield of the process under study, a multi-arm configuration containing five big and one small standard FOBOS modules in each arm was used. In order to select the CCT events accompanied almost isotropic neutron emission [18] the “neutron belt” consisting of 140 ^3He -filled neutron counters in the moderator was assembled in a plane perpendicular to the symmetry axis of the spectrometer which serves as the mean fission axis at the same time. The centre of the belt coincides with the location of the fission source.

The experiment Ex3 has been performed using the Correlation Mosaic E - T Array (COMETA). It is a double arm time-of-flight spectrometer which includes a MCP based “start” detector with the ^{252}Cf source inside, similar to that used in Ex1. Two mosaics of eight PIN diodes each and a “neutron belt” comprising 28 ^3He -filled neutron counters are used. Each PIN diode (2×2 cm of surface area) provides both energy and timing signals.

The most pronounced manifestation of the CCT as a missing mass event is a bump (Fig. 1) in the two dimensional of the mass-mass correlation plot [19]. In this distribution of the fission fragment masses the bump occurs in one of the spectrometer arms with dispersive media (M_1), whereas it is absent in the analogous variable for the second arm (M_2). The bump is marked by the arrow in Fig. 1a. We see two great bumps due to binary fission; the pronounced vertical and horizontal intensities are due to binary fission fragments scattered from the entrance support grid for the windows of the gas detectors. The FF mass correlation plot similar to that obtained in Ex1 (Fig. 1a) is shown in Fig. 2a. Projections of this distribution both on the M_1 axis and on the $M_s = \text{const}$ directions are presented in Fig. 2b, c. They are compared with the analogous spectra from the experiments Ex1 including the result from the $^{235}\text{U}(n_{\text{th}}, f)$ reaction [19]. The bump in the projected FF mass correlation data in Fig. 2b is centered on mass (68–70) amu, associated with magic isotopes of Ni. This bump will be called below as the “Ni”-bump. The bump marked by the arrow in Fig. 2a looks less pronounced as compared to that obtained in Ex1 (Fig. 1a). This can be partially explained by a worse mass resolution due to the wide-aperture avalanche counter used as “start” detectors in Ex2, instead of the MCP based detector in Ex1. Projections for Ex2 are shown in the “difference” version, i.e. as a difference of the

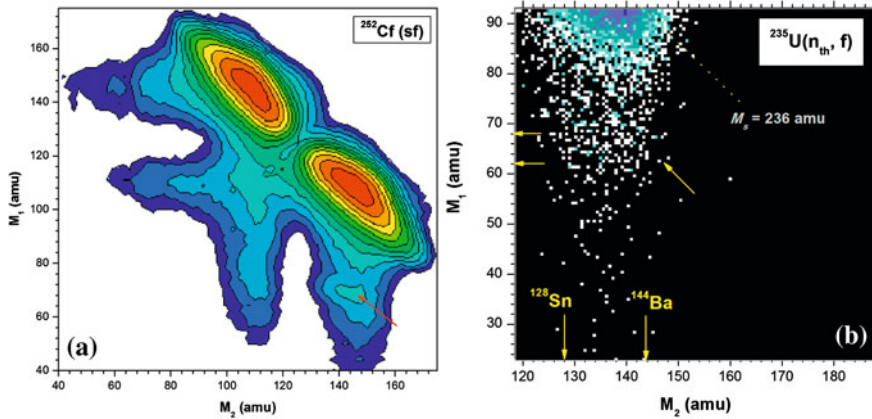


Fig. 1 **a** Contour map (in logarithmic scale, the steps between the lines are approximately a factor 2.5) of the mass-mass distribution of the collinear fragments of $^{252}\text{Cf}(\text{sf})$, detected in coincidence in the two opposite arms of the FOBOS spectrometer. The specific bump in arm1 is indicated by an arrow. **b** The region of the mass distribution for the FFs from the reaction $^{235}\text{U}(n_{\text{th}}, \text{f})$ around the bump. The bump is bounded by magic clusters (marked by corresponding symbols near the axes). The tilted arrow shows a valley between the ridges $M_1 + M_2 = 210$ amu of $M_s = \text{const}$. See text for details

tail regions in arm1 and in arm2, respectively. Overall a good agreement is observed in the position of the peaks in Fig. 2b, c for all three experiments.

The methodically quite different experiment Ex3 shows results, which confirm our previous results concerning the structures in the missing mass distributions. In this case there is no tail due to scattering from material in front of the E -detectors. Figure 3 shows the region of the mass distribution for the FFs from $^{252}\text{Cf}(\text{sf})$ around the “Ni”-bump ($M_1 = 68\text{--}80$ amu, $M_2 = 128\text{--}150$ amu). The structures are seen in the spectrometer arm facing the source backing only. No additional selection of the fission events has been applied in this case; the experiment has no background from scattered FFs. A rectangular-like structure below the locus of binary fission is bounded by magic nuclei (their masses are marked by the numbered arrows) namely ^{128}Sn (1), ^{68}Ni (2), ^{72}Ni (3). Two tilted diagonal lines with $M_s = 196$ amu and $M_s = 202$ amu (marked by number 4) start from the partitions 68/128 and 68/134, respectively. In experiment Ex1 [19], Fig. 6, similar sub-structures have been seen for masses $M_s = 204, 208, 212, 214$ amu where they were revealed indirectly by the applying of the second derivative filter, but in the absolutely statistically reliable distribution (“Ni”-bump) processed. Bearing in mind essential difference in the geometry of blocking mediums in Ex1 and Ex3 to be decisive for the relative experimental yields of the CCT modes with different angular distributions between the fragments forming the fork flying in the same direction the preference of lighter partitions standing behind the tilted ridges in Ex3 is not strange.

Positions of the points in the lower part of Fig. 3 do not contradict to possible existence of all the ridges revealed in Ex1 if the following magic partitions are assigned to their beginnings: 70/134, 68/140, 68/144, 70/144.

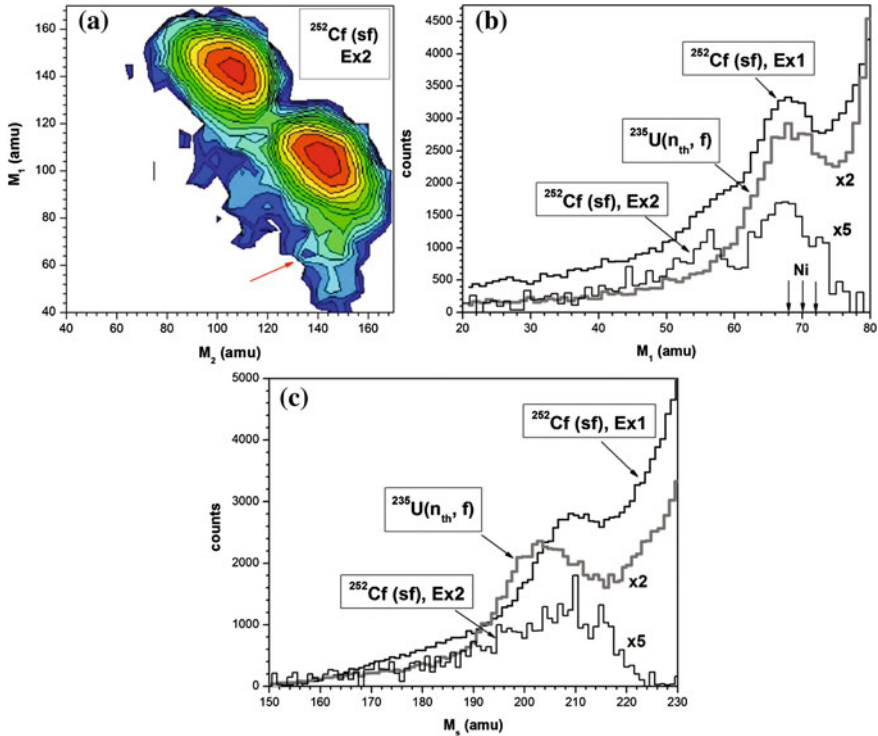


Fig. 2 Ex2. **a** Contour map of the mass-mass distribution (logarithmic scale, with lines approximately a factor 1.5) from a coincidence in the two opposite arms of Ex2. The bump in the spectrometer arm (arm1) facing the backing of the Cf source is marked by the *arrow*. **b** Projections onto the M_1 axis for comparison with the experiments Ex1, and with the results of the $^{235}\text{U}(n_{th}, f)$ reaction (Fig.1b) [1]. **c** Projections onto the direction $M_s = M_2 + M_1$. Ex1 is presented by two curves marked by the *arrows* 1 and 2 (*dotted*) for the arm1 and arm2, respectively

Thus, comparison of Ex1 and Ex3 which are absolutely different both by the detectors and mass calculation procedures used as well as the statistics collected delivers strong confirmation of the existence of tilted ridges $M_s = \text{const}$ linked with magic partitions. As can be inferred from Fig. 3, the yield of the FFs with the mass 128 amu, which is extremely low in conventional binary fission, is clearly seen. It means that scattered binary fragments in any case cannot give rise to this structure. A part of the plot just below the locus of the binary FFs is shown in a larger scale in the insert. The structure is bounded by the magic nuclei of ^{80}Ge , ^{78}Ni , ^{132}Sn , ^{144}Ba (their masses are marked by the arrows 5, 6, 7, 8, respectively).

The observations presented point to the fact that the CCT decay occurs in a variety of modes (mass combinations), which could not be distinguished in Ex1 without additional gating due to the large background from scattered FFs. Likely due to the difference in the parameters of the blocking mediums the yield of the “Ni”-bump in Ex3 does not exceed 10^{-3} per binary fission i.e. much less than in Ex1 and Ex2. At

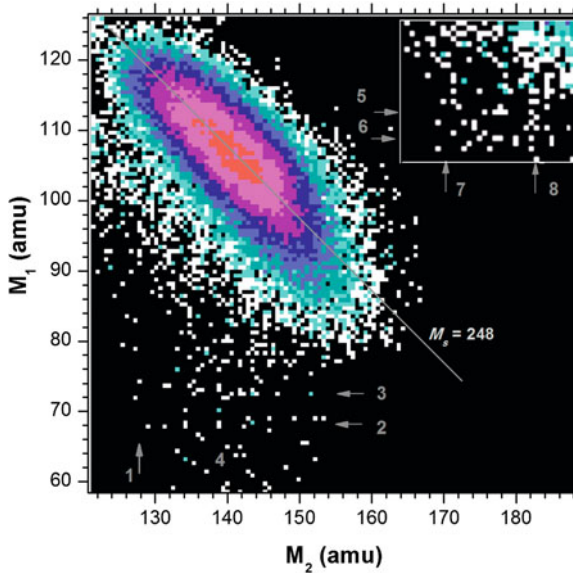
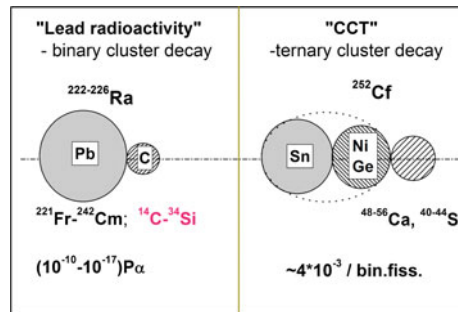


Fig. 3 Results of Ex3: The region of the mass-mass distribution for the FFs from ^{252}Cf (sf) around the CCT bump (Figs. 1a, 2a). No additional gates were applied. A part of the plot just below the locus of binary FFs produces the rectangular structure seen before. It is shown in the *insert* in a larger scale

Fig. 4 Cluster scheme for the comparison of the lead radioactivity with collinear cluster tri-partition



the same time with the absence of scattered FFs in Ex3, allowed the observation of the internal structure, without any additional cleaning of the FF mass distribution.

We would like to stress that one of the decay modes manifesting itself via tilted ridges $M_s = \text{const}$ can be treated as a new type of cluster decay as compared to the well-known heavy ion or lead radioactivity. Key features of both are summed up in Fig. 4. The relatively high CCT yield can be understood if one assumes collective motion through hyper-deformed pre-scission shapes of the mother systems, which is supported by the fact that the linear arrangement realizes the lowest Coulomb potential energies of three clusters. We also emphasize that the Q -values for ternary fission

are by 25–30 MeV more positive, again due to the formation of magic fragments, as in binary fission. The ternary fission process must be considered to proceed sequentially, with two neck ruptures in a short time sequence characteristic for binary fissions.

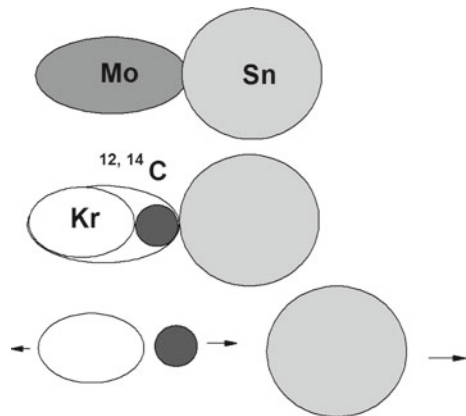
3 Light Ion Accompanied CCT Modes

Specific CCT modes were observed in the data from the reaction $^{235}\text{U}(n_{\text{th}},f)$ [20]. The experiment was performed at the mini-FOBOS setup. This is a two arm time-of-flight-fission fragment-energy spectrometer based on standard detector modules of the 4π FOBOS spectrometer [17].

The discussed data are related to almost collinear tri-partition of $^{236}\text{U}^*$ nucleus due to the limited spectrometer aperture (the maximum deviation of the lightest fragment from the fission axis cannot exceed 14°). As was shown in [20] there is a possibility to discriminate fission events distorted due to scattering of the fragments involved by means of special gating. Corresponding procedure is based on the experimental values of the time-drift of the track formed by the detected fragment in the ionization chamber. We have find [20] that almost in all events selected the light ion (light charged particle) is registered in coincidence with a fragment from the light group of mass distribution of fission fragments observed in conventional binary fission.

The obtained experimental information can be generalized in the context of the following scenario of the two-stage decay of $^{236}\text{U}^*$: Being sufficiently elongated, the system clusterizes, forming the di-nuclear system (Fig. 5) from two magic clusters. Upon further elongation, the deformed light magic cluster (Mo) clusterizes with partitioning of the light charged particle (carbon nucleus) and the magic remainder (Kr). The process of collinear cluster tri-partition according to a similar scenario in $^{236}\text{U}^*$ may take place not only in valleys of mass asymmetric but also mass symmetric shapes [21]. To the best of our knowledge, the described effect was not

Fig. 5 Illustration of the scenario of collinear cluster tri-partition accompanied by the emission of the light ion



observed earlier in works on the polar emission of light charged particles, which is probably associated with the excessive thicknesses of the dE detectors used to identify the charge of light charged particles [22].

4 New Aspects from Neutron Gated Data

The experiments with coincident neutrons were motivated by the expectation that the center fragment is connected to an isotropic neutron source of increased (as compared to binary fission) multiplicity linked with the CCT. For this reason a selection of the fission events with an increased number of detected neutrons was studied.

Corresponding results obtained at the COMETA setup are presented in Fig. 6.

A rectangular structure bounded by the magic clusters is seen. This structure is invisible in the initial ungated distribution, because it is located very close to the centre of the conventional binary fission events, as can be seen from the comparison of Fig. 6 with Fig. 1a. The structure manifests itself exclusively thanks to the difference of the neutron sources for the fragments appearing in both binary fission and CCT, respectively. These two decay modes must differ in the neutron multiplicity or/and in their angular distributions of the emitted neutrons in order to provide the higher registration efficiency for neutrons linked with the CCT channel. The value

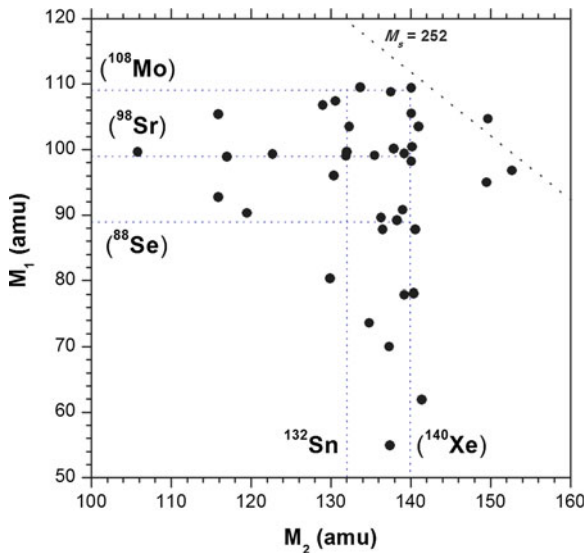


Fig. 6 Ex3 ($n = 3$, and $w1$): Results obtained at the COMETA setup: mass-mass distribution of the FFs from $^{252}\text{Cf}(\text{sf})$ under the condition that three neutrons ($n = 3$) were detected in coincidence and an additional selection with the gate $w1$ in the (V1-E1) distribution below the loci of conventional binary fission was applied [18]

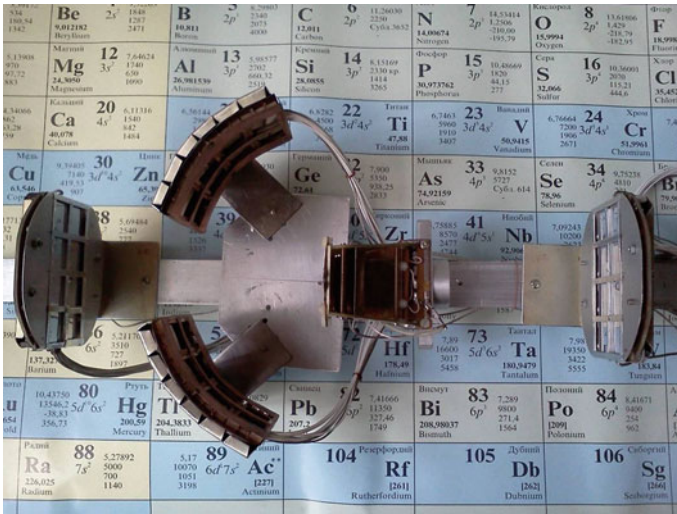


Fig. 7 Photo of the COMETA-2 setup

of the excitation energy at the scission point known from the experiment let come to conclusion that the neutron source that the structures in Fig. 6 differs from this in binary fission just by the angular distribution of the emitted neutrons.

5 To a Unified Model of Ternary Decays of Low Excited Nuclei

For the moment three different types of ternary decays of low excited nuclei are known, namely, conventional ternary fission, polar emission and CCT. It seems there is a deep link between the polar emission and CCT, at least with the CCT accompanied by a light charged particle. It would be extremely interesting to compare all three ternary decays in the frame of the unified experimental approach. We are planning to do this by means of step by step increasing of the aperture of the COMETA spectrometer and the first step has been already done. Recently COMETA-2 set up (Fig. 7) was put into operation at the FLNR of the JINR.

It contains four mosaics of Si semiconductor detectors of eight diodes each and the micro channel plates based “start” detector with the ²⁵²Cf inside. The FFs detectors are surrounded by the “neutron belt” which was used previously at the COMETA spectrometer. Processing of the data of the test run is in progress.

6 Conclusions

1. A new bright phenomenon is observed—CCT.
2. CCT is due to the pre-formation of at least two magic clusters, deformed as well. The CCT modes based on these combinations are more preferable.
3. There is an open field for the systematic study of CCT since it may bring us new knowledge on the fission process and clustering in cold nuclear matter.

References

1. O. Hahn, F. Strassmann, *Naturwissenschaften* **27**, 89 (1939)
2. K.A. Petrzhak, G.N. Flerov, *J. Phys.*, USSR **3**, 275 (1940)
3. L. Meitner, O. Frisch, *Nature* **143**, 239 (1939)
4. C.F. von Weizsäcker, *Z. Phys.* **96**, 431 (1935)
5. W.J. Swiatecki, in *Proceeding of the Second UN Conference on the Peaceful Uses of Atomic Energy, Geneva*, vol. 15, p. 651 (1958)
6. V.M. Strutinsky et al., *Nucl. Phys.* **46**, 639 (1963)
7. H. Diehl, W. Greiner, *Phys. Lett. B* **45**, 35 (1973)
8. H. Diehl, W. Greiner, *Nucl. Phys. A* **229**, 29 (1974)
9. D.N. Poenaru et al., *Phys. Rev. C* **59**, 3457 (1999)
10. M.L. Muga, *Phys. Rev. Lett.* **11**, 129 (1963)
11. P. Schall, *Phys. Lett. B* **191**, 339 (1987)
12. F. Ginnenwein, *Nucl. Phys. A* **734**, 213 (2004)
13. S.A. Karamian et al., *Jad. Fiz.* **5**, 959 (1963)
14. P. Glässel et al., *Z. Phys. A* **310**, 189 (1983)
15. Yu.V. Pyatkov et al., in *Proceeding of the International Conference of Nuclear Physics “Nuclear Shells—50 Years”* (World Scientific, Singapore, 2000), p. 301
16. Yu.V. Pyatkov et al., in *Proceeding of the International Symposium on Exotic Nuclei (EXON-2001)* (World Scientific, Singapore, 2002), p. 181
17. H.-G. Ortlepp et al., *Nucl. Instrum. Methods A* **403**, 65 (1998)
18. Yu.V. Pyatkov et al., *Eur. Phys. J. A* **48**, 94 (2012)
19. Yu.V. Pyatkov et al., *Eur. Phys. J. A* **45**, 29 (2010)
20. Yu.V. Pyatkov, *Bulletin of the Russian academy of sciences. Physics* **75**, 949 (2011)
21. V.V. Pashkevich et al., *Int. J. Mod. Phys. E* **18**, 907 (2009)
22. E. Piasecki et al., *Nucl. Phys. A* **255**, 387 (1975)